photonics

MDPI

Article

Comparison of Theoretical Impact of Lateral Translation and Cyclotorsion on Residual Aberrations in Refractive Surgery

Samuel Arba Mosquera [1,*] and Shwetabh Verma [2]

[1] Medical Affairs, SCHWIND Eye-Tech-Solutions GmbH, D-63801 Kleinostheim, Germany
[2] Research and Development, SCHWIND Eye-Tech-Solutions GmbH, D-63801 Kleinostheim, Germany; shwetabh.verma@eye-tech.net
* Correspondence: samuel.arba.mosquera@eye-tech.net

Abstract

Purpose: To quantitatively compare the theoretical optical effects of lateral translation and cyclotorsion on residual aberrations following refractive surgery using a common wavefront-based metric. **Methods:** Corneal wavefront data from 2543 eyes without previous ocular surgery were analyzed at a 6 mm pupil diameter. Zernike coefficients through the seventh radial order were transformed using an analytical framework for translated and rotated wavefronts. Lateral translation was simulated along the X-axis from −1.00 to +1.00 mm, and cyclotorsion from −15° to +15°. For each simulated condition, relative residual RMS was calculated as the residual wavefront RMS relative to the original wavefront RMS and averaged across eyes. Translation and cyclotorsion producing comparable relative residual RMS values were estimated using shape-preserving piecewise cubic Hermite interpolation. Combined translation and rotation were also evaluated. **Results:** Relative residual RMS increased approximately symmetrically with the magnitude of both alignment errors, with a substantially greater sensitivity to lateral translation. A relative residual RMS of 5% corresponded to approximately 0.09 mm of translation or 2.8° of cyclotorsion, whereas 25% relative residual RMS corresponded to approximately 0.42 mm or 14.1°, respectively. The translation–rotation relationship was nonlinear. When both errors were present, relative residual RMS increased with increasing magnitude of either error, while retaining greater sensitivity to translation. **Conclusions:** In this theoretical analysis, substantially smaller lateral translations produced relative residual RMS comparable to that produced by larger cyclotorsion errors. Expressing both errors through a common metric provides a quantitative framework for interpreting their relative optical effects. The resulting relationship represents a theoretical optical comparison and does not establish clinical alignment tolerances or equivalent visual effects.

Keywords: refractive surgery; cyclotorsion; treatment decentration; wavefront aberration; Zernike polynomials; wavefront-guided surgery; ocular alignment

Check for updates

Received: 17 September 2026
Revised: 20 November 2026
Accepted: 23 November 2026
Published: 26 November 2026

Copyright: © 2026 by the authors. Licensee MDPI, Basel, Switzerland. This article is an open access article distributed under the terms and conditions of the Creative Commons Attribution (CC BY) license.

1. Introduction

The optical quality of the human eye can be characterized by its wavefront aberrations, which are commonly represented using Zernike polynomials [1]. Zernike decomposition provides a standardized framework for describing the magnitude and distribution of ocular aberrations and is widely used in wavefront measurement and wavefront-guided refractive procedures [2,3]. Although several commercial devices are available to measure ocular aberrations with reasonable accuracy, differences between measurements obtained using

different commercial systems have also been reported [4,5]. The statistical properties of Zernike expansions in the normal human population have been investigated extensively [6]. Low-order aberrations, particularly defocus and astigmatism, are the predominant terms in normal eyes, whereas among higher-order aberrations, coma, trefoil, and spherical aberration are prominent components. Coma and trefoil may represent approximately 6% and spherical aberration approximately 2% of the total wavefront aberration variance [7].

In refractive surgery, accurate alignment between the intended treatment and the ocular coordinate system is important for minimizing residual aberrations. Misalignment can arise from translational and rotational components. Lateral translation represents a displacement between the intended treatment center and the ocular reference position, whereas cyclotorsion represents rotation of the eye around its optical axis. Both forms of misalignment can alter the spatial relationship between the planned correction and the underlying ocular wavefront and thereby result in residual aberrations [8]. An important question is therefore whether the impact of these alignment errors can be compared to each other based on a common metric. For refractive surgery, such an analysis could provide a clinically intuitive means of interpreting the relative theoretical optical effects of these two alignment errors. This would place two otherwise different types of alignment error on a common scale when considering their potential contribution to residual aberrations.

The magnitude and clinical relevance of translational misalignment depend, in part, on the reference axis selected for treatment centration. The appropriate centration reference in refractive surgery remains controversial, with subject-fixated, non-coaxially sighted corneal light reflex and pupil-centered procedures representing the two commonly used approaches [9]. The offset between the pupil center and the corneal vertex, estimated through the coaxially sighted corneal light reflex, has generally been reported to be less than 0.5 mm in normal subjects [10]. However, substantially larger offsets have been reported in patients with keratoconus [11]. A significant displacement of the line of sight has been observed in keratoconus and has been related to the location of the corneal cone and to induced vertical coma measured by aberrometry. Misalignment relative to the selected centration axis can induce aberrations including defocus, astigmatism, and coma [12]. Thus, clinically relevant translational errors can arise from differences between ocular reference axes and the selected treatment centration.

The optical effects of cyclotorsion have also been extensively investigated, both clinically and theoretically [13]. Arba-Mosquera et al. [14] described the theoretical effects of pure cyclotorsional errors during refractive surgery and developed a method to determine the average cyclotorsion occurring during refractive surgery without the use of a cyclotorsion tracker. In simulations based on 76 consecutive right-eye treatments, applying cyclotorsion to ablations based purely on Zernike decomposition resulted in residual aberrations within the same Zernike modes but with different magnitudes and orientations. Their findings indicated that the effect of cyclotorsion misalignment can be analyzed in terms of the magnitude and orientation of individual Zernike modes. The effect of cyclotorsion on individual modes was found to depend on angular frequency rather than radial order. They further reported that the theoretical impact of cyclotorsion errors on coma and spherical aberration was smaller than that associated with decentration or edge effects [14].

Direct comparisons between translational and cyclotorsion misalignment have also been reported. Wang et al. [15] calculated residual wavefront aberrations caused by clinically measured cyclotorsion misalignment and decentration in 58 eyes of 38 patients using an iris-registration system. On average, centration error induced 4.9 times, 2.8 times, and 8.7 times higher values of total aberrations (second to sixth orders), lower-order aberrations (LOAs; second order), and higher-order aberrations (HOAs; third to sixth orders), respectively, than cyclotorsion misalignment [15]. These findings indicate that, for the

clinically observed errors evaluated in that study, decentration can produce substantially greater residual aberrations than cyclotorsion. However, such comparisons quantify the relative impact of the two error types within particular clinical datasets; they do not establish a direct relationship between a specific amount of translation and a specific amount of cyclotorsion that produces the same residual aberration. Furthermore, relatively few studies have examined this relationship across a large population or over a broad range of translational and cyclotorsion errors, including extreme values. The present theoretical analysis complements the clinical findings of Wang et al. [15] by comparing translation and cyclotorsion using a common wavefront-based metric, rather than duplicating their clinical assessment. A quantitative comparison of these two alignment errors requires a mathematical framework capable of representing both translation and rotation within the same wavefront description. Lundström and Unsbo [16] presented a comprehensive analytical method for transforming Zernike coefficients under concentric scaling, translation of the pupil center, and rotation, using matrix-based transformations. This framework provides a means of theoretically analyzing how translation and rotation alter the individual Zernike coefficients and, consequently, the resulting wavefront aberration. It therefore provides an appropriate basis for evaluating the relative effects of lateral translation and cyclotorsion using a common metric. The implementation used in the present study is based on this published framework and is not a newly developed or study-specific implementation. It has previously been used in our published work [17,18] and is also incorporated into the commercial SCHWIND CAM treatment-planning software.

In the present descriptive study, we applied the transformation framework of Lundström and Unsbo [16] to a large database of 2543 normal eyes that had never undergone ocular surgery. Lateral movement was simulated as translation of the Zernike coefficients, whereas cyclotorsion was simulated as their rotation. Residual aberration was quantified using relative RMS of the second through seventh Zernike orders as a common metric. The resulting translation–rotation relationship was evaluated across a broad range of simulated alignment errors, including simultaneous translation and rotation, on a large population of normal eyes. The aim was to provide a quantitative framework for comparing the theoretical optical effect of alignment error, thereby facilitating the understanding of relative optical significance of translational and cyclotorsion errors encountered during refractive surgery, independent of the specific treatment modality.

2. Methods

2.1. Study Population and Wavefront Data

Corneal wavefront data from 2543 normal eyes that had never undergone ocular surgery were obtained from Augenzentrum Recklinghausen, Recklinghausen, Germany. Wavefront data were available at a 6 mm pupil diameter. The mean age of the study population was 31 ± 9.4 years. The mean spherical equivalent defocus was −1.17 ± 2.5 D, and the mean cylinder was −0.55 ± 1.0 D.

For each eye, the corneal wavefront was represented using Zernike coefficients through the seventh radial order, corresponding to 36 Zernike terms. For the Zernike polynomials, the conventions specified by the OSA/ANSI standards and the corresponding ISO standards were used. Piston and the two tilt terms were set to zero before transformation. Accordingly, the analysis focused on the second through seventh Zernike orders. Potential coupling contributions from piston and tilt into higher-order modes during coordinate translation were not considered. The complete 36-term Zernike coefficient vector was retained for the subsequent transformations and residual RMS calculations.

2.2. Zernike Coefficient Transformation

An algorithm was implemented in Scilab (SW version 6.1.1) (Scilab Enterprises, Vélizy-Villacoublay, France) based on the analytical transformation methods described by Lundström and Unsbo [16]. For each eye, the original Zernike coefficient vector was used as the input to the simulation. Lateral translation and ocular rotation were mathematically represented as translation and rotation, respectively, of the Zernike coefficient representation of the corneal wavefront.

For each simulated condition, the transformed Zernike coefficients were obtained as the output of the algorithm. The residual Zernike coefficient for each term was calculated as the difference between the original and transformed coefficients:

$$\Delta Z_j = Z_{j,\ original} - Z_{j,\ transformed}$$

where (j) represents each of the 36 Zernike terms. The sign of the residual does not affect the RMS calculation. The coordinate origin was defined as the center of the 6 mm analysis pupil. Translation was defined along the X-axis, with the positive X-direction pointing towards the patient's right side and the positive Y-direction pointing towards the patient's feet. Rotation was defined around the optical Z-axis, with positive values indicating counterclockwise rotation and negative values indicating clockwise rotation.

2.3. Calculation of Relative Residual RMS

For each eye and each simulated condition, the RMS of the residual Zernike coefficient vector was calculated and normalized to the RMS of the original Zernike coefficient vector. The relative residual RMS was calculated as

$$Relative\ residual\ RMS = \sqrt{\frac{\sum_{j=1}^{N}\left(\Delta Z_j\right)^2}{\sum_{j=1}^{N}\left(\Delta Z_{j,Original}\right)^2}}$$

where $N = 36$. The resulting value was expressed either as a decimal ratio or as a percentage. Thus, the relative residual RMS represents the residual wavefront RMS produced by a given simulated alignment error relative to the RMS of the original wavefront for that eye. This normalization provides a dimensionless measure of the relative aberration change, allowing the effects of translation and cyclotorsion to be compared on a common relative scale. Importantly, the RMS of the difference wavefront is not equivalent to the difference between the RMS values of the original and transformed wavefronts. Therefore, calculating the residual RMS directly from the difference wavefront provides a measure of the aberration change induced by the transformation. Relative residual RMS was calculated separately for each eye and each simulation condition and subsequently averaged across 2543 eyes. Thus, the reported population value represents the mean of eye-specific relative RMS values.

2.4. Effect of Pure Translation

The effect of lateral translation in the absence of rotation was evaluated by transforming the Zernike coefficients along the X-axis. Although the transformation algorithm permits independent translation along the X- and Y-axes, the present analysis was restricted to translation along the X-axis to provide a consistent one-dimensional representation of translational error.

Translation was simulated from −1.00 to +1.00 mm in increments of approximately 0.33 mm, resulting in translation values of −1.00, −0.66, −0.33, 0, +0.33, +0.66, and +1.00 mm. This range was selected to encompass relatively large lateral decentrations, while the sampling interval represented a practical compromise between the number of simulated conditions and resolution. No rotational transformation was applied during these simula-

tions. The mean relative residual RMS was calculated for each translation value across the 2543 eyes.

2.5. Effect of Pure Rotation

The effect of rotation in the absence of translation was evaluated by rotating the Zernike coefficient vector around the optical axis. Rotation was simulated from −15° to +15° in 5° increments (−15°, −10°, −5°, 0°, +5°, +10°, and +15°). This range was selected to encompass the majority of clinically encountered cyclotorsional deviations, while the 5° increment represented a practical compromise between the number of simulated conditions and sampling resolution. No translational transformation was applied during these simulations. The mean relative residual RMS was calculated for each rotational angle across the 2543 eyes.

2.6. Comparison of Translation and Rotation

The relationships between the magnitude of translation and rotation and their corresponding mean relative residual RMS values were used to compare the theoretical optical effects of the two alignment errors.

For each simulated translation or rotation condition, the corresponding mean relative residual RMS represented the magnitude of the residual aberration relative to the original wavefront RMS. The translation and rotation response relationships were therefore expressed using the same dimensionless metric, allowing the magnitude of one type of alignment error to be compared with that of the other.

Translation and rotation conditions associated with comparable mean relative residual RMS values were identified. Where relevant, for RMS values falling between two simulated conditions, the corresponding translation or rotation was estimated using shape-preserving piecewise cubic Hermite interpolation (PCHIP). The resulting relationships were graphically represented to provide a direct comparison between lateral translation and cyclotorsion in terms of their theoretical residual aberration. For graphical presentation, simulated values were plotted as individual markers, with straight-line segments connecting consecutive simulation points. These connecting segments serve as a visual representation of the simulated data and are not used for the PCHIP-based interpolation. For illustrative comparison, relative residual RMS levels of 5% and 25% were selected to represent two different magnitudes of residual aberration, allowing the translation–rotation relationship to be examined at both lower and higher levels of relative residual RMS. These values were not intended to represent clinical thresholds or acceptable alignment tolerances.

2.7. Effect of Simultaneous Rotation and Translation in Aberrations

In clinical settings, translational and rotational alignment errors may occur simultaneously rather than as isolated phenomena. To analyze their combined effects, simulations were performed in which both transformations were applied simultaneously to the original Zernike coefficient representation of each eye. Rotation was simulated from −15° to +15° in 5° increments. For each rotational angle, simultaneous horizontal translation along the X-axis was simulated from −0.66 to +0.66 mm in approximately 0.33 mm increments. The resulting Zernike coefficients were then used to calculate the residual relative RMS for each combination of translation and rotation.

3. Results

3.1. Effect of Pure Rotation

The mean relative residual RMS increased approximately linearly with the magnitude of pure rotation, from 0% at 0° to approximately 9%, 18%, and 27% at ±5°, ±10°, and ±15°, respectively (Figure 1). The response was approximately symmetric for positive

and negative rotation. Error bars in Figure 1 represent the standard deviations across the 2543 eyes. The corresponding 95% confidence intervals of the mean were approximately 8.8–9.2%, 17.5–18.4%, and 25.9–27.2% at ±5°, ±10°, and ±15°, respectively. The distribution of individual-eye responses for each rotational condition is additionally presented as box-and-whisker plots in Figure 2.

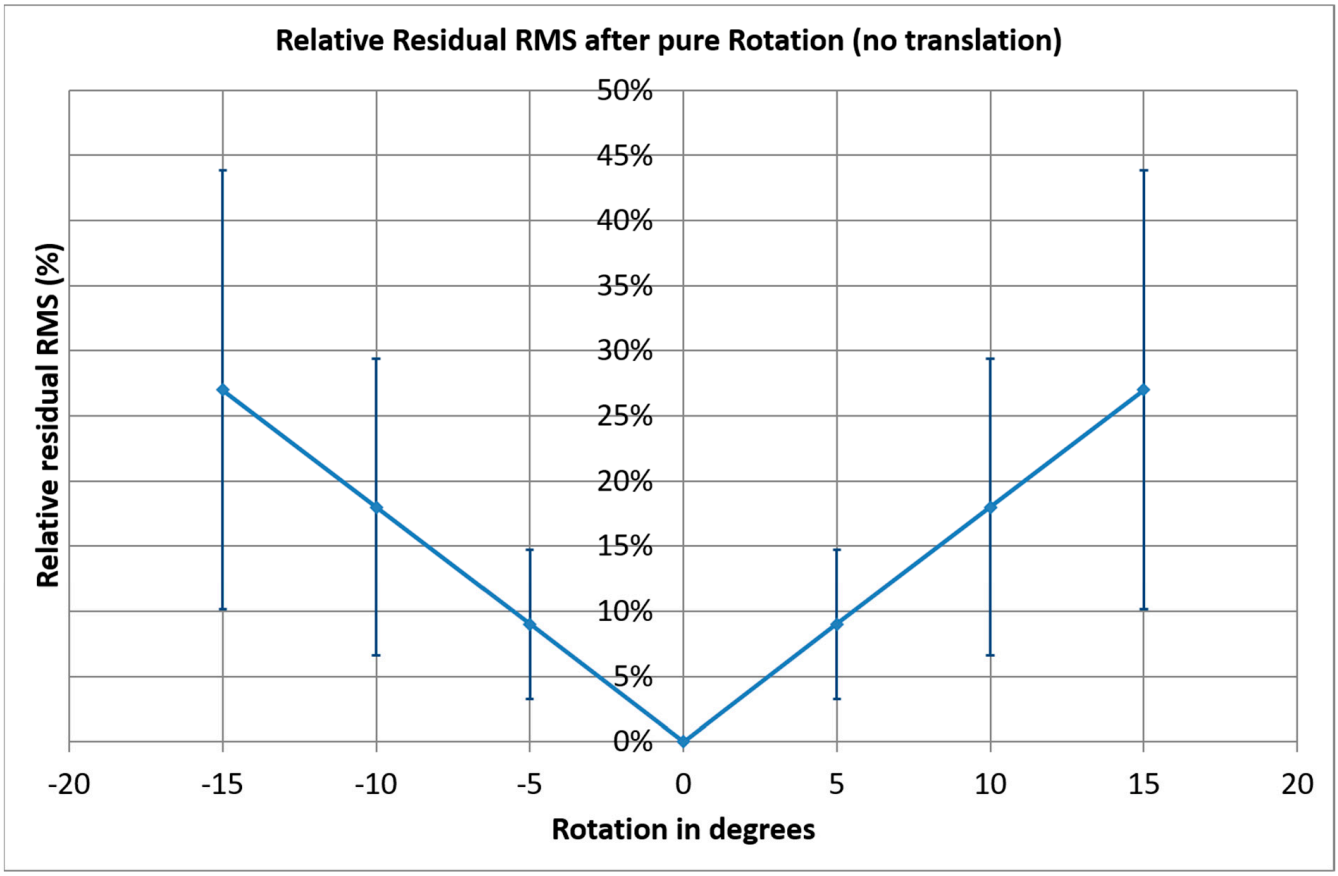

Figure 1. Effect of pure rotation on relative residual RMS. Mean relative residual RMS as a function of cyclotorsion rotation from −15° to +15° in the absence of translation. Error bars represent ±1 standard deviation across the 2543 eyes. The response was approximately symmetric for positive and negative rotation.

3.2. Effect of Pure Translation

For pure translation, mean relative residual RMS increased from 0% at 0 mm to approximately 19%, 43%, and 80% at −0.33, −0.66, and −1.00 mm, respectively, and 19%, 43%, and 79% at the corresponding positive translations (Figure 3). Error bars in Figure 3 represent the standard deviations across the 2543 eyes. The corresponding 95% confidence intervals of the mean ranged from 18.6–19.7% at ±0.33 mm, 42.0–44.6% at −0.66 mm and 41.6–44.2% at +0.66 mm, and 76.9–82.2% at −1.00 mm and 76.2–81.6% at +1.00 mm. The distributions of individual-eye responses for each translation condition are additionally presented as box-and-whisker plots in Figure 4.

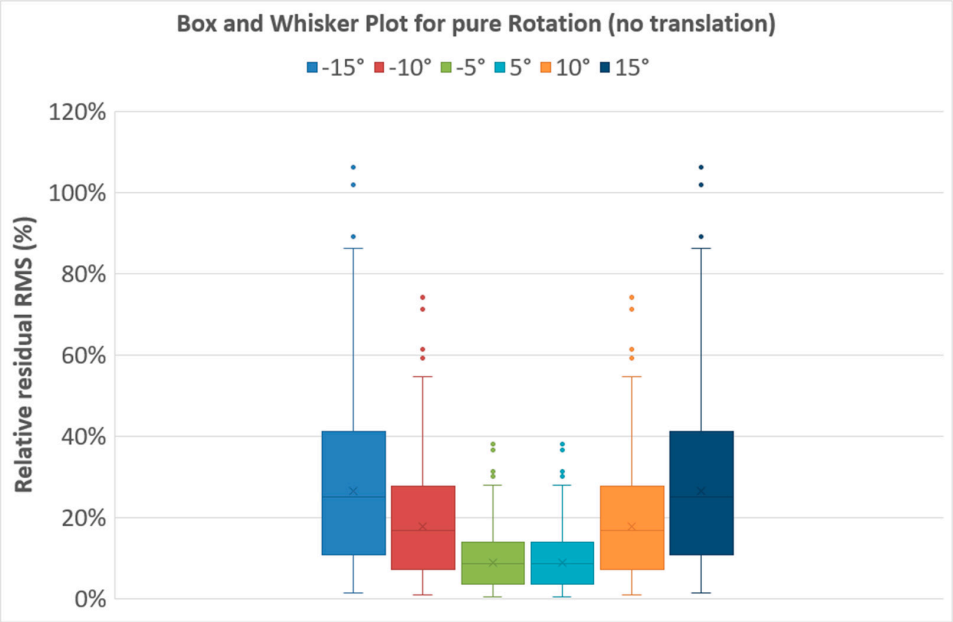

Figure 2. Distribution of relative residual RMS across the 2543 eyes for pure cyclotorsion from −15° to +15° in the absence of translation. The zero-rotation condition is omitted because it produces zero residual RMS for all eyes. Boxes represent the interquartile range (25th–75th percentiles), horizontal lines indicate the median, and crosses (×) indicate the mean. Whiskers extend to the most extreme data points within 1.5 times the interquartile range (IQR), while individual points beyond the whiskers indicate outliers.

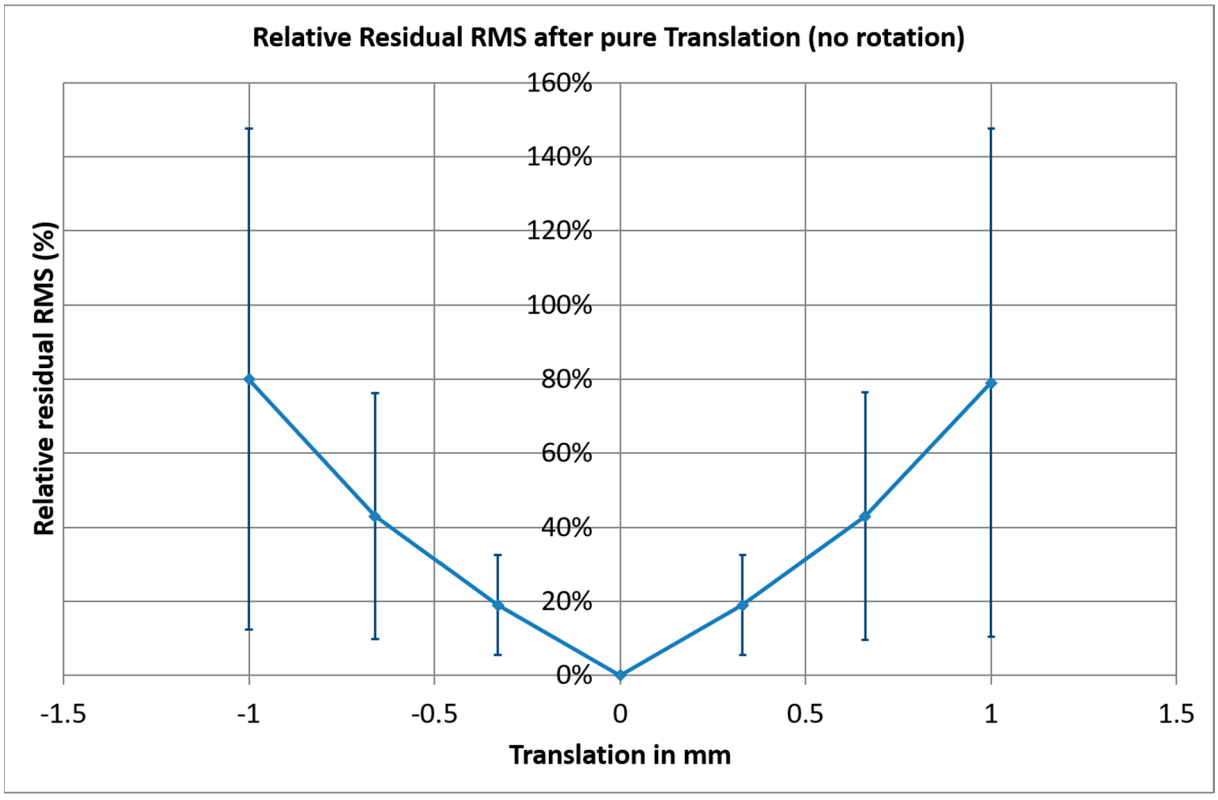

Figure 3. Effect of pure lateral translation on relative residual RMS. Mean relative residual RMS as a function of horizontal translation along the X-axis from −1.00 to +1.00 mm in the absence of rotation. Error bars represent ±1 standard deviation across the 2543 eyes. The response was approximately symmetric for positive and negative translation.



Figure 4. Distribution of relative residual RMS across the 2543 eyes for pure lateral translation along the X-axis from −1.00 to +1.00 mm in the absence of rotation. The zero-translation condition is omitted because it produces zero residual RMS for all eyes. Boxes represent the interquartile range (25th–75th percentiles), horizontal lines indicate the median, and crosses (×) indicate the mean. Whiskers extend to the most extreme data points within 1.5 times the interquartile range (IQR), while individual points beyond the whiskers indicate outliers.

3.3. Comparison of Translation and Rotation

The pure translation and pure rotation response curves were compared using relative residual RMS as the common metric (Figure 5). The relative residual RMS values associated with translation ranged from 0% at 0 mm to approximately 80% at −1.00 mm and 79% at +1.00 mm, while those associated with rotation ranged from 0% at 0° to approximately 27% at ±15° (Figure 5).

The relationship between translation and rotation was nonlinear. The linear relationship in Figure 5 is shown for reference. The comparison demonstrated a markedly greater change in relative residual RMS per unit of lateral translation than per unit of cyclotorsion. Thus, relatively small translational displacements produced residual RMS values comparable to those associated with substantially larger rotational errors. Using PCIH interpolation, a relative residual RMS of 5% corresponded to approximately 0.09 mm of translation or 2.8° of rotation. At a higher relative residual RMS of 25%, the corresponding values were approximately 0.42 mm of translation and 14.1° of rotation (Figure 5).

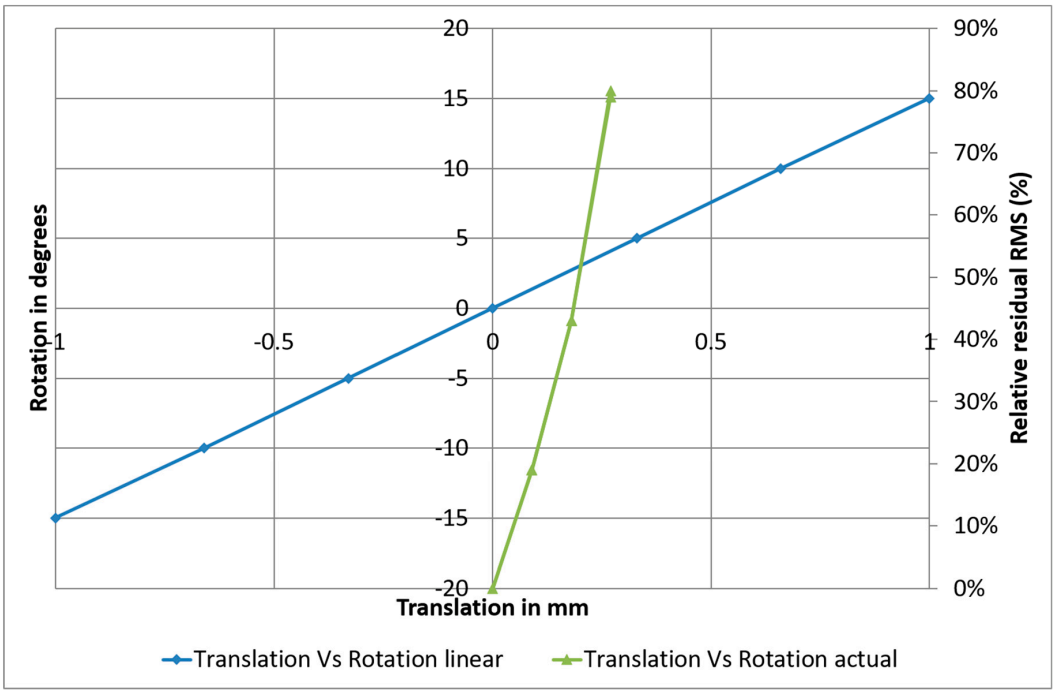

Figure 5. Relationship between translation and rotation based on relative residual RMS. Pure translation and rotation are represented on the basis of the mean relative residual RMS produced by each alignment error. The curves allow translation and cyclotorsion producing comparable relative residual RMS to be identified using a common metric. The straight line represents a linear reference obtained by plotting the seven simulated translation values (−1.00 to +1.00 mm) against the seven corresponding rotation values (−15° to +15°), illustrating a proportional relationship for comparison. It does not represent a model of the underlying optical transformation. The actual relationship is represented by the curves connecting the simulated values.

3.4. Effect of Simultaneous Rotation and Translation in Aberrations

The combined effect of translation and rotation was evaluated across translation values from −0.66 to +0.66 mm and rotation values from −15° to +15°. The resulting relative residual RMS values are presented graphically for fixed translation values in Figure 6 and for fixed rotation values in Figure 7.

Across the simulated range, the relative residual RMS increased with increasing magnitude of either translation or rotation. At zero translation, the relative residual RMS values corresponded to those observed for pure rotation: approximately 9%, 18%, and 27% at ±5°, ±10°, and ±15°, respectively (Figure 6). Similarly, at zero rotation, the values corresponded to those observed for pure translation, with approximately 19% and 43% relative residual RMS at ±0.33 and ±0.66 mm, respectively (Figure 7).

When both translation and rotation were present, the relative residual RMS increased with the magnitude of both alignment errors. The combined simulations retained the greater sensitivity to translational displacement observed in the pure-error analysis. For example, at ±0.33 mm translation, the relative residual RMS was approximately 19% at 0° rotation and increased to approximately 22%, 27%, and 33% at ±5°, ±10°, and ±15°, respectively (Figure 6). At ±0.66 mm translation, the corresponding values were approximately 43%, 44%, 47%, and 52% at 0°, ±5°, ±10°, and ±15°, respectively (Figure 6).

When the results were viewed for fixed rotational errors, a similar increase in relative residual RMS with increasing translation was observed (Figure 7). At 5° rotation, the relative residual RMS increased from approximately 9% at zero translation to approximately 21% and 44% at ±0.33 and ±0.66 mm translation, respectively. At 10° rotation, the corre-

sponding values were approximately 18%, 27%, and 47%, while at 15° rotation they were approximately 27%, 33%, and 52%, respectively (Figure 7).

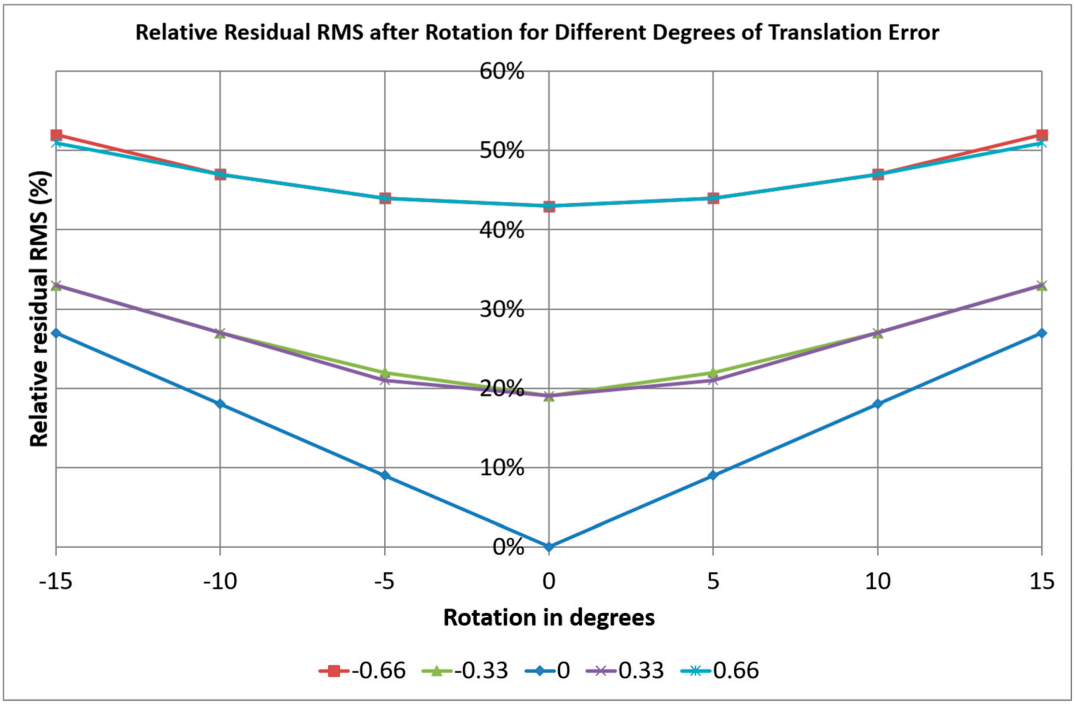

Figure 6. Relative residual RMS as a function of cyclotorsion for different levels of lateral translation. Mean relative residual RMS following simultaneous translation and rotation across the simulated ranges of −0.66 to +0.66 mm and −15° to +15°, respectively. Each curve represents a fixed translation value.

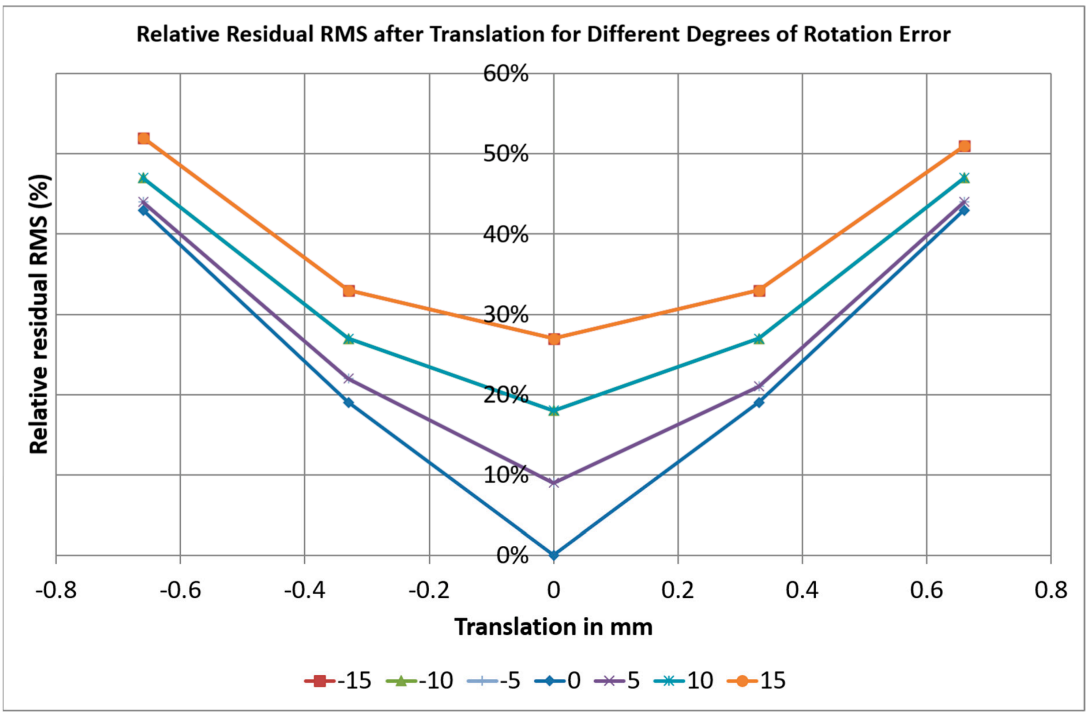

Figure 7. Relative residual RMS as a function of lateral translation for different levels of rotation. Mean relative residual RMS following simultaneous translation and rotation across the simulated ranges of −0.66 to +0.66 mm and −15° to +15°, respectively. Each curve represents a fixed rotational value.

4. Discussion

4.1. Principal Findings

Normalization to the original wavefront RMS reduces the dependence of the relative residual RMS on the absolute magnitude of the baseline aberrations. However, it does not eliminate the influence of the individual aberration composition, as the response to translation and cyclotorsion depends on the spatial distribution and relative contributions of the individual Zernike components. The observed inter-eye variability, reflected in the standard deviations and distributions of the relative residual RMS values, illustrates that eyes exposed to the same alignment error can exhibit substantially different responses. Consequently, eyes with similar baseline RMS values may exhibit different responses to the same alignment error. The results therefore represent the average response across the investigated population rather than implying identical behavior for every individual eye.

The present analysis demonstrated a substantially greater sensitivity of residual wavefront RMS to lateral translation than to cyclotorsion. Using relative residual RMS as a common metric, a residual RMS of 5% corresponded, based on PCIH, to approximately 0.09 mm of lateral translation or 2.8° of cyclotorsion. At a higher relative residual RMS of 25%, the corresponding values were approximately 0.42 mm of translation and 14.1° of cyclotorsion. Thus, over the simulated range, substantially smaller translational displacements were required to produce the same relative residual RMS as rotational errors. This provides a quantitative means of expressing the relative optical sensitivity to these two forms of alignment error rather than comparing translation and rotation only as separate physical quantities.

The finding is consistent in direction with previous clinical observations. Wang and Koch evaluated residual aberrations associated with clinically measured cyclotorsion misalignment and decentration during wavefront-guided excimer laser corneal ablation and reported that centration error produced, on average, 4.9-fold higher total aberrations, 2.8-fold higher lower-order aberrations, and 8.7-fold higher higher-order aberrations than cyclotorsion misalignment [15]. Although the numerical relationships cannot be directly compared because the present study and the study by Wang and Koch used different populations, error distributions, analytical approaches, and aberration metrics, the agreement in the direction of the effect is notable. The present analysis extends this clinical observation by providing a common RMS-based framework in which a specific magnitude of translation can be related to a specific magnitude of cyclotorsion producing a comparable residual aberration.

4.2. Clinical Relevance of the Simulated Cyclotorsion

Cyclotorsion movements have been reported before and during laser refractive surgery and can influence the relationship between the intended treatment and the ocular orientation [13,19]. The magnitude of cyclotorsion varies considerably among eyes. Ciccio et al. reported a mean cyclotorsion of 4.05 ± 2.9° with a range of 0.5° to 17.5° in 1019 consecutive eyes undergoing wavefront-guided corneal ablation [20]. The upper end of this reported clinical range therefore approaches the ±15° range evaluated in the present analysis. The use of an extended simulation range consequently allows the translation–rotation relationship to be examined beyond the magnitude encountered in the majority of eyes while remaining within the range of cyclotorsion errors that has been clinically observed.

Several methods have been developed to identify or compensate for cyclotorsion misalignment during refractive surgery, including limbal marking, active eye tracking, and iris registration [21–24]. Chen et al. demonstrated that limbal marking can reduce the magnitude of cyclotorsion error [23], while iris-registration systems have been developed to register the treatment to the ocular orientation and compensate for rotational misalign-

ment [21,22]. Active eye-tracking technology has also been investigated as a means of improving alignment during corneal laser surgery [24]. These approaches illustrate the clinical importance attributed to rotational alignment, particularly when the treatment contains orientation-dependent components.

However, the theoretical optical effect of cyclotorsion should not be equated directly with a measurable clinical visual benefit from cyclotorsion compensation. Moshirfar et al., for example, compared LASIK performed with and without iris registration using the VISX CustomVue platform and found no statistically significant differences in visual acuity, astigmatic correction, or induction of higher-order aberrations under their study conditions [25]. Similar observations have been reported in the literature reviewed by Arba-Mosquera and Verma [13]. These findings emphasize that an alignment error may produce a theoretical change in the wavefront without necessarily resulting in a detectable difference in a particular clinical visual endpoint. The present analysis therefore addresses the optical consequence of alignment error, rather than predicting the magnitude of clinical visual benefit obtained by correcting that error.

The magnitude of cyclotorsion measured clinically should also be interpreted carefully. Prickett et al. demonstrated that the total iris rotation observed between sitting and supine positions contains both a cyclotorsion component and non-cyclotorsion components related to posture and head position [26]. In their analysis of 310 eyes of 155 patients, total rotation ranged from −8.30° to +9.20°, whereas the calculated cyclotorsion component ranged from approximately −3.15° to +7.40° [26]. The authors therefore emphasized that total measured rotation does not necessarily represent pure cyclotorsion in an individual eye. The rotational values in the present analysis represent pure rotation around the optical axis and should consequently not be interpreted as directly equivalent to every clinically measured change in iris orientation.

4.3. Clinical Relevance of Lateral Translation

The translational results provide a complementary perspective on the importance of treatment centration in refractive surgery. The present simulations indicate that relatively small lateral displacements can produce a residual RMS comparable to that associated with considerably larger rotational errors. This is clinically relevant because lateral displacement may arise from differences between ocular reference axes, treatment centration strategies, pupil position, or treatment alignment [9,27–30].

The choice of reference for treatment centration has remained an important consideration in refractive surgery. Different reference positions, including the entrance pupil center, line of sight, corneal vertex, and coaxially sighted corneal light reflex, have been investigated and debated [9,27–30]. Chang and Waring, for example, described the subject-fixated coaxially sighted corneal light reflex as a clinical marker for centration of refractive treatments and devices [9]. Applegate et al. further emphasized the importance of fixation, pupil center, and reference axis when interpreting ocular wavefront measurements and retinal image quality [27]. Consequently, some component of lateral displacement may arise not from a failure of the laser system itself but from the relationship between the selected treatment reference and the ocular coordinate system.

The magnitude of translation identified in the present theoretical analysis is also within the scale of alignment errors that have been considered clinically relevant in previous theoretical work. Bueeler et al. investigated the lateral alignment accuracy required for aberration-sensing and wavefront-guided corneal ablation and reported that, for a 7.0 mm pupil, a lateral alignment accuracy of approximately 0.07 mm or better was required to achieve the diffraction limit in 95% of normally aberrated eyes, whereas approximately 0.2 mm was sufficient for a 3.0 mm pupil under their criterion [8]. These values are of the

same order as the approximately 0.091 mm translation associated with 5% relative residual RMS in the present analysis. Direct numerical comparison should nevertheless be avoided because the endpoints, pupil diameters, and analytical approaches were different. The comparison is instead useful in demonstrating that the translational magnitudes associated with the present theoretical analysis fall within a range that has previously been considered optically relevant.

The effect of decentration on ocular aberrations has also been demonstrated in theoretical and clinical studies. Padmanabhan et al. investigated eyes with decentered ablations and demonstrated changes in their wavefront aberration profiles [31]. Theoretical analyses have similarly described the relationship between treatment decentration and induced wavefront aberrations following corneal laser refractive surgery [32]. These observations provide clinical context for the present finding that lateral translation can produce a relatively large residual RMS with comparatively small physical displacement.

4.4. Translation and Cyclotorsion on a Common Optical Scale

A principal advantage of expressing both alignment errors through relative residual RMS is that translation and rotation can be compared using a common optical metric. A millimeter of translation and a degree of rotation are otherwise fundamentally different physical quantities and cannot be meaningfully compared directly. By considering the residual aberration generated by each error, Figure 5 instead asks what magnitude of each alignment error produces a comparable optical consequence.

This comparison provides a different perspective on the clinical findings reported by Wang and Koch [15]. Their analysis compared the residual aberrations associated with clinically measured centration errors and cyclotorsion misalignment and found substantially greater aberrations associated with centration error. The present analysis approaches the same general question from a complementary direction: rather than comparing the residual aberrations associated with clinically observed errors, it determines how much of each alignment error is required to produce the same relative residual RMS. The consistency in the direction of the findings supports the observation that, under the conditions investigated, lateral translation produced greater relative residual RMS than cyclotorsion for the corresponding simulated magnitudes.

Importantly, this relationship does not imply that cyclotorsion compensation is clinically unimportant. Cyclotorsion can change the orientation of astigmatic and higher-order corrections, and its importance depends on the magnitude and structure of the treatment [13,19]. Rather, the present analysis provides a quantitative context in which the magnitude of a rotational error can be considered relative to a translational error having a comparable theoretical effect on residual wavefront RMS.

4.5. Combined Translation and Cyclotorsion

In clinical refractive surgery, translational and rotational alignment errors may occur simultaneously rather than as isolated phenomena. The simultaneous simulations in the present analysis demonstrated that the relative residual RMS increased as either component of the alignment error increased (Figures 6 and 7). Thus, even when the individual contribution of cyclotorsion is smaller than that of translation, rotational error may contribute additional residual aberration when it occurs together with lateral displacement.

The combined analysis is relevant to the practical interpretation of alignment errors because treatment centration and cyclotorsion compensation are not necessarily independent aspects of the surgical alignment process. A treatment may therefore be exposed to both positional displacement and rotational mismatch. The two-dimensional representation in

Figures 6 and 7 provides a means of considering these errors together rather than evaluating them independently.

The combined simulations should nevertheless be interpreted in the context of the theoretical nature of the present analysis. The relative residual RMS describes the magnitude of the residual Zernike wavefront produced by the modeled alignment errors but does not directly predict postoperative visual performance. Furthermore, the combined response may depend on the underlying aberration structure of an individual eye, meaning that the same nominal translation and rotation need not produce identical residual aberration distributions in different eyes.

4.6. Clinical Interpretation

The principal clinical value of the present analysis is not the establishment of a new tolerance limit for translation or cyclotorsion. Rather, it provides a simple framework for placing the two alignment errors on a common optical scale. This may be particularly useful when considering alignment requirements in wavefront-guided and other aberration-sensitive corneal refractive procedures. The results suggest that small lateral displacements warrant particular attention because the translational magnitude required to generate a given relative residual RMS was consistently smaller than the rotational magnitude required to produce the same effect. This theoretical observation is consistent with clinical studies demonstrating substantial residual aberration associated with decentration, and greater aberration associated with centration errors than with cyclotorsion misalignment [8,15,31].

The results should not, however, be interpreted as establishing a specific residual RMS percentage as a threshold for clinically significant visual degradation. The 5% and 25% values used in the present comparison serve as examples for illustrating the translation–rotation relationship rather than as proposed clinical tolerance limits. The clinical significance of a particular residual aberration depends on its modal composition, pupil diameter, pre-existing aberrations, treatment characteristics, and the visual system's response to the resulting retinal image.

4.7. Limitations

The present analysis has several limitations. First, the residual aberrations were derived theoretically from transformations of Zernike coefficients rather than measured following an actual refractive procedure. The analysis therefore represents the theoretical optical consequence of the simulated alignment error rather than a direct measurement of postoperative ocular aberration.

Second, the analysis was based on relative monochromatic wavefront RMS and therefore does not directly represent visual performance. The visual process is more complex than an image-projection system and includes chromatic aberration, neural processing, and neural adaptation, which were beyond the scope of the present analysis. In particular, subjective visual symptoms associated with residual aberration may not correlate directly with total RMS because the spatial distribution and type of aberration also influence retinal image quality.

Third, the analysis was based on normal eyes with a 6 mm pupil and therefore may not directly represent eyes with substantially different corneal aberration profiles, pupil diameters, or corneal pathology. While the relative effect of cyclotorsion is expected to remain largely independent of pupil diameter, the relative effect of a given translational displacement may decrease with increasing pupil diameter, owing to both the increase in baseline wavefront RMS and the smaller displacement relative to the pupil radius. These effects were not investigated at other pupil diameters in the present study.

Fourth, translation was simulated along the X-axis, although the transformation framework permits independent translation along the X- and Y-axes. The magnitude of the residual aberration induced by translation may depend on its direction relative to the spatial orientation of the underlying aberration components. Consequently, the reported translation–rotation relationship and corresponding translation values are specific to X-axis translation and may differ for other directions of lateral displacement. Furthermore, piston and tilt were excluded from the input Zernike coefficient vector before applying the transformations. Although these terms do not represent image-degrading aberrations in the same manner as higher-order aberrations, coordinate translation can theoretically redistribute their contributions into higher-order modes. Such coupling contributions were not considered in the present analysis. The translational and rotational ranges were also selected to provide a broad theoretical comparison and should not be interpreted as representing the distribution of errors encountered in routine clinical practice.

Finally, relative residual RMS provides a common quantitative metric but does not capture the complete spatial or perceptual consequences of the residual aberration. Two residual wavefronts with similar RMS may have different distributions among Zernike modes and consequently different effects on retinal image quality or subjective visual symptoms. Consequently, comparable relative residual RMS values do not imply similar spatial or modal structure of the residual aberration. The translation–rotation relationship should therefore be regarded as a theoretical optical comparison rather than a direct clinical threshold for acceptable alignment.

4.8. Conclusions

Despite these limitations, the present analysis provides a simple theoretical framework to quantitatively analyze the relationship between lateral translation and cyclotorsion that is otherwise difficult to obtain from clinical observations alone. The finding that substantially smaller translational errors produce residual RMS values comparable to those produced by larger cyclotorsion errors is consistent with previous theoretical and clinical observations of the greater sensitivity of residual aberration to decentration [8,15,32]. By expressing the two alignment errors through a common relative residual RMS metric, the analysis provides a quantitative basis for comparing their theoretical optical effects under the investigated conditions.

The resulting relationship may therefore be useful as a theoretical guide for clinicians and treatment-system developers when considering the relative consequences of translational and cyclotorsion alignment errors. It does not replace clinical assessment of visual outcomes or establish absolute alignment tolerances but rather provides a quantitative framework for understanding how the two forms of misalignment compare in terms of their predicted residual wavefront aberration. Furthermore, the framework may also be useful when comparing alignment specifications of refractive surgery systems. Rather than considering them as independent quantities expressed in different physical units, their potential optical consequences can be considered through the residual aberration generated by each error.

Author Contributions: Conceptualization, S.A.M. and S.V.; methodology, S.A.M. and S.V.; formal analysis, S.A.M. and S.V.; investigation, S.V.; resources, S.A.M. and S.V.; data curation, S.A.M. and S.V.; writing—original draft preparation, S.V.; writing—review and editing, S.A.M. and S.V.; visualization, S.A.M. and S.V.; supervision, S.A.M.; project administration, S.A.M. All authors have read and agreed to the published version of the manuscript.

Funding: This research received no external funding.

Institutional Review Board Statement: Not applicable.

Informed Consent Statement: Not applicable.

Data Availability Statement: The data underlying the results presented in this paper are not publicly available at this time but may be obtained from the authors upon reasonable request.

Conflicts of Interest: The authors declare no conflicts of interest. The authors declare no competing interests. Both authors are employed by the company SCHWIND eye-tech solutions GmbH, Germany. There are no conflicts of interest between any of the authors and the company SCHWIND eye-tech solutions GmbH, Germany.

References

1. Thibos, L.N.; Applegate, R.A.; Schwiegerling, J.T.; Webb, R.; VSIA Standards Taskforce Members. Standards for reporting the optical aberrations of eyes. In Proceedings of the Vision Science and Its Applications, Santa Fe, NM, USA, 11–14 February 2000.
2. Campbell, C.E. Analysis of wavefront-guided corrections to see if they fully correct ocular aberrations. *J. Opt. Soc. Am. A Opt. Image Sci. Vis.* **2006**, *23*, 1559–1565. [CrossRef] [PubMed]
3. Zernike, F. Beugungstheorie des schneidenver-fahrens und seiner verbesserten form, der phasenkontrastmethode. *Physica* **1934**, *1*, 689–704. [CrossRef]
4. Cade, F.; Cruzat, A.; Paschalis, E.I.; Santo, L.E.; Pineda, R. Analysis of four aberrometers for evaluating lower and higher order aberrations. *PLoS ONE* **2013**, *8*, e54990. [CrossRef] [PubMed]
5. de Jong, T.; Sheehan, M.; Dubbelman, M.; Koopmans, M.; Jansonius, N. Shape of the anterior cornea: Comparison of height data from 4 corneal topographers. *J. Cataract Refract. Surg.* **2013**, *39*, 1570–1580. [CrossRef] [PubMed]
6. Porter, J.; Guirao, A.; Cox, I.G.; Williams, D.R. Monochromatic aberrations of the human eye in a large population. *J. Opt. Soc. Am. A* **2001**, *18*, 1793–1803. [CrossRef] [PubMed]
7. Villegas, E.A.; Alcón, E.; Artal, P. Impact of positive coupling of the eye's trefoil and Coma in retinal image quality and visual acuity. *J. Opt. Soc. Am. A Opt. Image Sci. Vis.* **2012**, *29*, 1667–1672. [CrossRef] [PubMed]
8. Bueeler, M.; Mrochen, M.; Seiler, T. Maximum permissible lateral decentration in aberration-sensing and wavefront-guided corneal ablations. *J. Cataract Refract. Surg.* **2003**, *29*, 257–263. [CrossRef] [PubMed]
9. Chang, D.; Waring, W. The subject-fixated coaxially sighted corneal light reflex: A clinical marker for centration of refractive treatments and devices. *Am. J. Ophthalmol.* **2014**, *158*, 863–874. [CrossRef] [PubMed]
10. Mosquera, S.A.; Verma, S.; McAlinden, C. Centration axis in refractive surgery. *Eye Vis.* **2015**, *2*, 4. [CrossRef] [PubMed]
11. Miháltz, K.; Kránitz, K.; Kovács, I.; Takács, A.; Németh, J.; Nagy, Z.Z. Shifting of the line of sight in keratoconus measured by a hartmann-shack sensor. *Ophthalmology* **2010**, *117*, 41–48. [CrossRef] [PubMed]
12. Bühren, J.; Yoon, G.; Kenner, S.; MacRae, S.; Huxlin, K. The effect of optical zone decentration on lower- and higher-order aberrations after photorefractive keratectomy in a cat model. *Investig. Ophthalmol. Vis. Sci.* **2007**, *48*, 5806–5814. [CrossRef] [PubMed]
13. Mosquera, S.A.; Verma, S. Effects of torsional movements in refractive procedures. *J. Cataract Refract. Surg.* **2015**, *41*, 1752–1766. [CrossRef] [PubMed]
14. Arba-Mosquera, S.; Merayo-Lloves, J.; Ortueta, D. Clinical effects of pure cyclotorsional errors during refractive surgery. *Investig. Ophthalmol. Vis. Sci.* **2008**, *49*, 4828–4836. [CrossRef] [PubMed]
15. Wang, L.; Koch, D.D. Residual higher-order aberrations caused by clinically measured cyclotorsional misalignment or decentration during wavefront-guided excimer laser corneal ablation. *J. Cataract Refract. Surg.* **2008**, *34*, 2057–2062. [CrossRef] [PubMed]
16. Lundström, L.; Unsbo, P. Transformation of Zernike coefficients: Scaled, translated, and rotated wavefronts with circular and elliptical pupils. *J. Opt. Soc. Am. A Opt. Image Sci. Vis.* **2007**, *24*, 569–577. [CrossRef] [PubMed]
17. Mosquera, S.A.; Verma, S. Numerical nonwavefront-guided algorithm for expansion or recentration of the optical zone. *J. Biomed. Opt.* **2014**, *19*, 088001. [CrossRef] [PubMed]
18. Mehrjoo, M.; Gatinel, D.; Malet, J.; Mosquera, S.A. A Closed-Form Analytical Conversion between Zernike and Gatinel–Malet Basis Polynomials to Present Relevant Aberrations in Ophthalmology and Refractive Surgery. *Photonics* **2024**, *11*, 883. [CrossRef]
19. Chang, J. Cyclotorsion during laser in situ keratomileusis. *J. Cataract Refract. Surg.* **2008**, *34*, 1720–1726. [CrossRef] [PubMed]
20. Ciccio, A.E.; Durrie, D.S.; Stahl, J.E.; Schwendeman, F. Ocular cyclotorsion during customized laser ablation. *J. Refract. Surg.* **2005**, *21*, S772–S774. [CrossRef] [PubMed]
21. Chernyak, D.A. From wavefront device to laser: An alignment method for complete registration of the ablation to the cornea. *J. Refract. Surg.* **2005**, *21*, 463–468. [CrossRef] [PubMed]
22. Qazi, M.A.; Pepose, J.S.; Sanderson, J.P.; Mahmoud, A.M.; Roberts, C.J. Novel objective method for comparing ablation centration with and without pupil tracking following myopic laser in situ keratomileusis using the bausch & lomb technolas 217A. *Cornea* **2009**, *28*, 616–625. [CrossRef] [PubMed]

23. Chen, X.; Stojanovic, A.; Stojanovic, F.; Eidet, J.R.; Raeder, S.; Øritsland, H.; Utheim, T.P. Effect of limbal marking prior to laser ablation on the magnitude of cyclotorsional error. *J. Refract. Surg.* **2012**, *28*, 358–362. [CrossRef] [PubMed]
24. Mrochen, M.; Eldine, M.S.; Kaemmerer, M.; Seiler, T.; Hütz, W. Improvement in photorefractive corneal laser surgery results using an active eye-tracking system. *J. Cataract Refract. Surg.* **2001**, *27*, 1000–1006. [CrossRef] [PubMed]
25. Moshirfar, M.; Chen, M.C.; Espandar, L.; Meyer, J.J.; Christensen, D.; Christiansen, S.M.; Dave, S.B.; Bedke, B.; Kurz, C. Effect of iris registration on outcomes of LASIK for myopia with the VISX CustomVue platform. *J. Refract. Surg.* **2009**, *25*, 493–502. [CrossRef] [PubMed]
26. Prickett, A.L.; Bui, K.; Hallak, J.; Bakhtiyari, P.; Cruz, J.; Azar, D.; Chamon, W. Cyclotorsional and non-cyclotorsional components of eye rotation observed from sitting to supine position. *Br. J. Ophthalmol.* **2015**, *99*, 49–53. [CrossRef] [PubMed]
27. Applegate, R.A.; Thibos, L.N.; Twa, M.D.; Sarver, E.J. Importance of fixation, pupil center, and reference axis in ocular wavefront sensing, videokeratography, and retinal image quality. *J. Cataract Refract. Surg.* **2009**, *35*, 139–152. [CrossRef] [PubMed]
28. Pande, M.; Hillman, J.S. Optical zone centration in keratorefractive surgery. Entrance pupil center, visual axis, coaxially sighted corneal reflex, or geometric corneal center? *Ophthalmology* **1993**, *100*, 1230–1237. [PubMed]
29. Reinstein, D.Z.; Archer, T.J.; Gobbe, M. Is topography-guided ablation profile centered on the corneal vertex better than wavefront-guided ablation profile centered on the entrance pupil? *J. Refract. Surg.* **2012**, *28*, 139–143. [CrossRef] [PubMed]
30. Arbelaez, M.C.; Vidal, C.; Arba-Mosquera, S. Clinical outcomes of corneal vertex versus central pupil references with aberration-free ablation strategies and LASIK. *Investig. Ophthalmol. Vis. Sci.* **2008**, *49*, 5287–5294. [CrossRef] [PubMed]
31. Padmanabhan, P.; Mrochen, M.; Viswanathan, D.; Basuthkar, S. Wavefront aberrations in eyes with decentered ablations. *J. Cataract Refract. Surg.* **2009**, *35*, 695–702. [CrossRef] [PubMed]
32. Fang, L.; Wang, Y.; He, X. Theoretical analysis of wavefront aberration caused by treatment decentration and transition zone after custom myopic laser refractive surgery. *J. Cataract Refract. Surg.* **2013**, *39*, 1336–1347. [CrossRef] [PubMed]

Disclaimer/Publisher's Note: The statements, opinions and data contained in all publications are solely those of the individual author(s) and contributor(s) and not of MDPI and/or the editor(s). MDPI and/or the editor(s) disclaim responsibility for any injury to people or property resulting from any ideas, methods, instructions or products referred to in the content.